Cross-shell excitations in ^{46}Ca studied with fusion reactions induced by reaccelerated rare isotope beam

J. Ash,[1, 2, *] H. Iwasaki,[1, 2] T. Mijatović,[1, 3] T. Budner,[1, 2] R. Elder,[4] B. Elman,[1, 2]
M. Friedman,[1] A. Gade,[1, 2] M. Grinder,[1, 2] J. Henderson,[5] B. Longfellow,[1, 2] A.
Revel,[1] D. Rhodes,[1, 2] M. Spieker,[1, 6] Y. Utsuno,[7] D. Weisshaar,[1] and C. Y. Wu[8]

[1] *National Superconducting Cyclotron Laboratory, Michigan State University, East Lansing, MI 48824, USA*
[2] *Department of Physics and Astronomy, Michigan State University, East Lansing, MI 48824, USA*
[3] *Ruđer Bošković Institute, HR-10002 Zagreb, Croatia*
[4] *Department of Physics and Engineering, Washington and Lee University, Lexington, VA 24450, USA.*
[5] *Department of Physics, University of Surrey, Guildford, GU2 7XH, United Kingdom*
[6] *Department of Physics, Florida State University, Tallahassee, Florida 32306, USA*
[7] *Advanced Science Research Center, Japan Atomic Energy Agency, Tokai, Ibaraki 319-1195, Japan*
[8] *Lawrence Livermore National Laboratory, Livermore, Ca 94550, USA*
(Dated: February 11, 2021)

Discovering unexplored high-spin states in neutron-rich nuclei can open up a new direction to study band structure and the associated shell structure in isospin-asymmetric many-body systems. However, experimental reach has so far been limited to neutron-deficient or stable nuclei which are preferentially produced in fusion reactions used in such studies. Here, we report the first gamma-ray spectroscopy with fusion reactions using a reaccelerated rare-isotope beam of ^{45}K performed at the ReA3 facility of the National Superconducting Cyclotron Laboratory. Using particle and gamma-ray coincidence techniques, three new higher-lying states around 6 MeV and five new gamma-ray transitions were identified for ^{46}Ca, suggesting three independent band structures formed from different particle-hole configurations. The rotational-like band built on the 0_2^+ state is established up to the tentatively assigned 6_2^+ state. New results are compared to large-scale shell model calculations, confirming the validity of the effective interaction describing particle-hole excitations across the Z=20 and N=28 shell gaps in the vicinity of doubly-magic ^{48}Ca.

The chain of calcium isotopes provides an ideal testing ground for nuclear structure models. Recent experimental and theoretical efforts have aimed at exploring the rapid evolution of the shell structure of these nuclei out to the neutron dripline [1–10]. The recent discovery of ^{60}Ca at N=40 implies that the Ca dripline should extend to at least ^{70}Ca [3]. Meanwhile, gamma-ray spectroscopy has identified new magic numbers of $N = 32$ and $N = 34$ for ^{52}Ca [4, 5] and ^{54}Ca [6] respectively, with confirmation from mass measurements [7, 8]. For ^{52}Ca, an unexpectedly large charge radius found in Ref. [9] has posed challenges for theoretical interpretation, while recent density functional theory has successfully reproduced the observed trends of charge radii from ^{36}Ca all the way to ^{52}Ca [10]. This theory also addressed the importance of continuum effects in understanding the structural evolution in the isotopic chain.

While the isospin frontier has been the focus of many recent efforts in nuclear structure studies, the study of medium- to high-spin states remains an important challenge for neutron-rich nuclei [11–15]. For calcium isotopes, studies of high-spin structures have reached ^{40,42}Ca [16, 17], with pronounced shape coexistence identified for the low-lying 0^+ states and multiple band structures, extending to 16^+ in ^{40}Ca. For ^{44}Ca, a negative-parity rotational band from 3^- to 13^- was proposed [18] based on the $J(J + 1)$ trend of its energy levels. Shape

coexistence is expected to persist in heavier calcium isotopes [19], where the energy relation between spherical and deformed states may evolve far from stability, as seen in other neutron-rich regions including along the $N = 20$ and $N = 50$ isotones [20–22]. Expanding our knowledge of these deformed bands in the Ca isotopes and characterizing their evolution toward doubly-magic ^{48}Ca and beyond would give insight into the interplay between isospin and angular momentum and allow one to test advanced theoretical models that have been developed to describe low-lying structure of neutron-rich Ca isotopes [1, 6, 10, 23–25].

Previous investigations into ^{46}Ca have not uncovered the underlying band structure of the nucleus. Through particle spectroscopy, several excited states have been identified, using for instance ^{44}Ca(t, p) [26], ^{48}Ca(p, t) [27], and ^{46}Ca(p, p') [28]. However, gamma-ray spectroscopy has generally been limited to studies of low-lying and low-spin states [29]. A recent β^--decay measurement has identified 42 new excited states in ^{46}Ca [30], but no band structures were observed due to the selective population of low-spin states by the β^- decay of ^{46}K with $J_{gs.}^\pi = (2^-)$. As shown in previous work for ^{40,44}Ca [16, 18], fusion-evaporation reactions can be used effectively to study band-structures due to selective population of high-spin states, particularly the yrast states; however, no stable beam and target combination is capable of reaching ^{46}Ca with sufficient intensity. With the advent of reaccelerator facilities, rare-isotope beams at Coulomb barrier energies have become available, allow-

ing us to take advantage of fusion reaction mechanisms with a novel combination of beam and target. The National Superconducting Cyclotron Laboratory (NSCL) is uniquely capable of delivering the high purity reaccelerated beams produced following projectile fragmentation using the combination of the A1900 fragment separator [31] and the reaccelerated beam facility (ReA3) [32]. This yields a chemistry-independent mechanism for the production and reacceleration of rare isotope beams. By employing this capability, knowledge of band structures composed of high-spin states in magic calcium isotopes will be extended to ^{46}Ca.

In this Letter, we report our result on ^{46}Ca by means of gamma-ray spectroscopy with fusion reactions induced by reaccelerated rare isotope beams from the ReA3 facility [32]. A primary beam of ^{48}Ca was produced in the Coupled Cyclotron Facility and fragmented on a beryllium target to produce ^{45}K using the A1900 fragment separator. The potassium beam was collected in a gas-stopper cell with helium gas and delivered to the NSCL's electron beam ion trap (EBIT) [33], where it was prepared for injection into ReA3 through charge breeding. The resulting rare-isotope beam impinged on a 5.8 mg/cm^2-thick natural lithium target at an energy of 4.66 MeV/nucleon and an average intensity of 9.8×10^4 pps. Beam energy after the target was estimated to be 2.1 MeV/nucleon, just above the Coulomb barrier of the ^{7}Li + ^{45}K system. Reaction products, including isotopes of calcium, scandium, and titanium, were primarily produced via the fusion-evaporation mechanism. In particular, ^{46}Ca was produced in the ^{7}Li(^{45}K,$\alpha 2n\gamma$)^{46}Ca reaction channel. Calculations using PACE4 [34] for this reaction indicated production cross sections of 80-110 mb over most of the target thickness.

The use of a thick lithium target is key to realizing the present measurement. First, a thicker target can partly offset the relatively low beam intensity of ^{45}K compared to intensities typically used for fusion reaction studies with stable beams. Second, the thick target, together with the energy dissipation of fusion reactions, allows for reaction products to stop in the target, emitting gamma rays in the laboratory frame if excited-state lifetimes are sufficiently long. This enables us to observe distinct peak structures without Doppler broadening. In addition, the present inverse-kinematics setup results in a strong kinematic focusing of the ^{46}Ca reaction products, allowing the Doppler-shift correction for short-lived states to be made assuming that the reaction products travel along the beam axis. This configuration also helps to reduce the β^- decay background associated with ^{45}K, because the unreacted beam particles pass through the target and decay further downstream.

Gamma rays were detected using the Segmented Germanium Array (SeGA), which consists of 16 high-purity Germanium detectors [35] arranged in a barrel configuration into forward and backward rings surrounding the beam pipe. Each detector has 32-fold segmentation, and the gamma-ray hit position is used for Doppler-shift
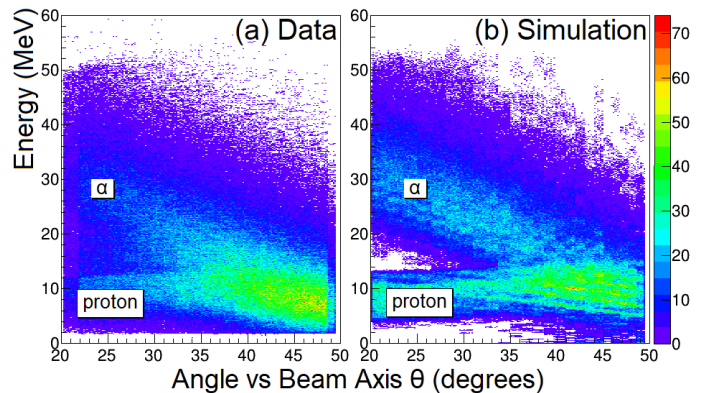

FIG. 1. Particle identification using energy and angle information from the silicon detector. The experimental result (a) is compared with simulations (b) based on PACE4 [34] and SRIM [36] calculations. The different behaviors of proton and alpha particles are well reproduced, including the maximum deposited energy of protons at around 12-14 MeV. The alpha gate used in Figs. 2 and 3 is defined for each angular bin by setting a minimum deposited energy to remove proton events.

correction, while the central contact signal determines the total gamma-ray energy absorbed by the detector. Photo-peak efficiencies of the array were measured with ^{152}Eu and ^{226}Ra sources to be 13.7% for 367.8-keV and 3.4% for 2448-keV gamma rays.

Charged particles recoiling out of the target were detected using an annular double-sided silicon detector, which provided partial selection of reaction channels. The arrangement was a modification of the JANUS setup used primarily for Coulomb excitation measurements at ReA3 [37]. The 1-mm thick S3-type detector was used for the present work and placed 3.1 cm downstream of the target. With an inner radius of 1.1 cm and an outer radius of 3.5 cm, the present setup covers polar angles θ from 20 to 50 degrees, where most of the recoil alpha particles from the production of ^{46}Ca were expected according to PACE4 calculations.

The design of the S3 detector allows for determination of the pixel of interaction through 24-fold radial and 32-fold azimuthal segmentation, corresponding to an angular resolution of about 1.5 degrees in polar (θ) and 11.3 degrees in azimuthal (ϕ) angles. Due to the inverse kinematics of the reaction, beam-like reaction products experienced forward focusing within 6 degrees relative to the beam axis, preventing them from reaching the active are of the silicon detector. To limit the detection of elastically scattered lithium, a 25-μm film of conductive mylar was placed between the target and the silicon detector. Instead of the standard particle identification based on ΔE-E, we measured the total energy deposited in the single thick detector in order to cover the recoiling particles emitted in a wide energy range. As demonstrated in Fig. 1(a), the angle-energy correlation shows that protons and alpha particles are distinguishable. The measured data were reproduced by the simulated results shown in Fig.
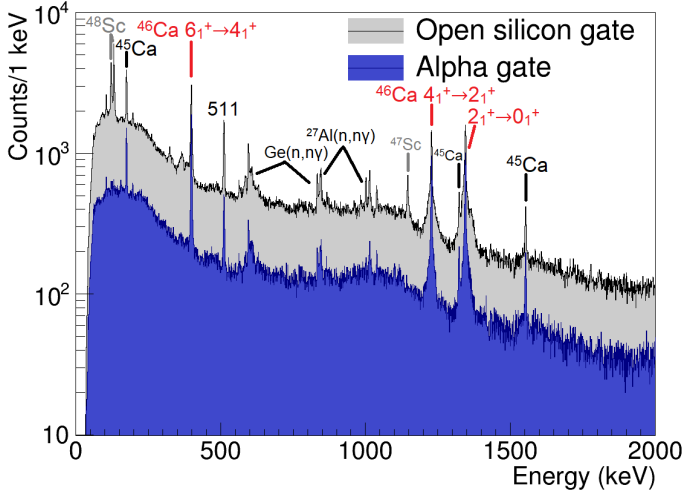
FIG. 2. Laboratory-frame particle-gamma coincidence spectrum. The plot compares the spectra with an open gate against the results when gating on alpha particles. Gamma-ray peaks from the reaction products ^{45,46}Ca and ^{47,48}Sc are labelled, as well as background from neutron-induced reactions.

FIG. 3. Doppler-corrected particle-gamma coincidence spectrum, with a gate on alpha particles. A fast transition known from ^{46}Ca is observed $\left(4_2^+ \to 2_1^+\right)$ [30], as well as newly identified peaks at 468 and 2715 keV and a peak structure at 309 keV, as seen in the inset. Laboratory-frame gamma rays are seen as doublets due to the different geometrical effects of the forward and backward SeGA detectors in the Doppler correction.

1(b), validating the present identification. The particle information provides a useful means to select reaction channels of interest.

In this study, excited states of ^{46}Ca were populated through the ^{7}Li(^{45}K,$\alpha 2n\gamma$)^{46}Ca reaction channel. Gamma rays were detected in coincidence with recoiling light particles. The resulting laboratory-frame and Doppler-corrected gamma-ray spectra are shown in Figs. 2 and 3, respectively. In Fig. 2, three gamma-ray peaks are evident that correspond to previously known transitions from the yrast 2_1^+, 4_1^+, and 6_1^+ states from ^{46}Ca. With the application of the alpha gate, these peaks survive, whereas the peaks from reaction products ^{47,48}Sc that should be associated with proton emission are eliminated from the spectrum. In the alpha-gated spectrum in Fig. 2, three peaks are also visible from the 174-, 1554-, and 1324-keV transitions in ^{45}Ca produced in the ^{7}Li(^{45}K,$\alpha 3n$)^{45}Ca reaction. The observed ^{46}Ca yrast-band cascade is summarized in Table I and illustrated in Fig. 5. The 6_1^+ state in ^{46}Ca is known to be isomeric with a mean lifetime τ of 15.0(7) ns [38, 39]; consequently, the decays occur after the nucleus has stopped in the target, presenting a distinct peak in the laboratory-frame spectrum. On the other hand, the broad shoulders observed on the higher and lower sides of the 4_1^+ and 2_1^+ peaks originate from Doppler-broadening associated with events where the states are populated promptly and gamma rays are emitted while the reaction product was still in flight. Background from neutron-induced reactions is also marked in the spectrum.

To identify gamma-ray transitions from short-lived states, a Doppler-shift correction was applied. Figure 3 presents the alpha-gated Doppler-corrected spectrum with $v/c = 6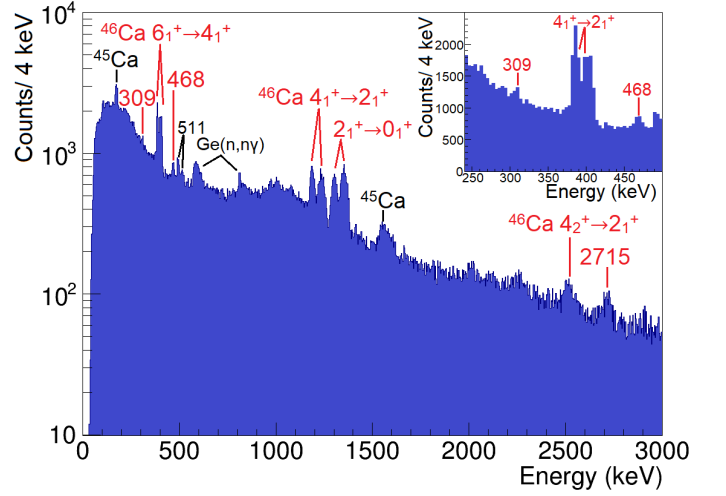.75\%$, assuming outgoing particles travel along the beam line. This velocity parameter was chosen to eliminate angular dependence of Doppler-corrected peak energies. The gamma-ray spectrum clearly presents newly identified peaks at 468 and 2715 keV, together with a peak structure at 309 keV. By gating on the transition for the 6_1^+ decay, these three new transitions were confirmed at 309, 468, and 2715 keV (Fig. 4(a)) and found to decay in a cascade above the 6_1^+ based on mutual coincidence relations. The 2715-keV gamma ray has a higher intensity than the other two gamma rays in the cascade, leading to the level scheme shown in Fig.5(a). The 309-keV and 468-keV transitions had equivalent intensities, so tentative placement in the level scheme was based on the ideal value of v/c for Doppler-shift correction ($v/c = 6.75\%$ for 309 keV and $v/c = 6.5\%$ for 469 keV). In addition, the gamma-ray peaks which correspond to decays from known states, including 5^- and (6_2^+) whose J^π were originally deduced from angular distributions [27], were newly observed in the present study using coincidence with the decay of the first excited state ($J^\pi = 2_1^+$), as shown in Fig. 4(b). In fact, when looking back at Fig. 3, a signature of the 6_2^+ decay is visible at 2006 keV, supporting the peak assignment. It should be noted that the energy gate used to select alpha particles is removed for Fig. 4 to maximize yields in ^{46}Ca gamma rays.

The conditions under which the new cascade was observed limit the possibilities of the spin and parity of the states among the cascade. All three gamma rays shown in Fig. 4(a) required Doppler-correction in order to be identified and thus were emitted in flight, corresponding to fast ($\tau < 10$ ps) decays. For the 5689-keV state, the
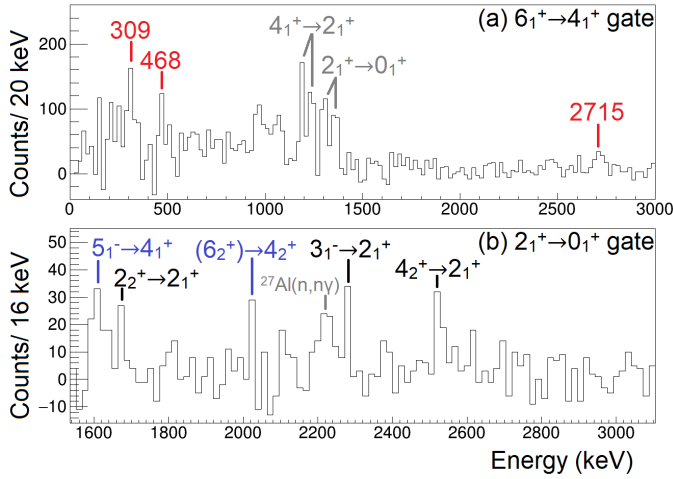
FIG. 4. Background-subtracted particle-gamma-gamma co-incidence gated on 399-keV (a) and 1346-keV (b) gamma rays confirmed new ^{46}Ca transitions. New transitions to (un)known states are labeled in blue (red). The counts around 900-1100 keV in (a) are remnants of the Compton edges of the 4_1^+ and 2_1^+ decays.

2715-keV transition directly populates the 6_1^+ state, and other transitions to lower-spin ($J < 6$) states were not observed. This non-observation indicates a high spin value for the 5689-keV state, above $J = 6$, leaving the natural parity assignments of 7^- or 8^+. For the other two transitions, their relatively low energies and short limit on their lifetimes exclude the possibility of E2 or higher multipolarity. Assuming a conservative upper limit on their lifetime of 10 ps, transition strengths have corresponding lower limits of $B(E1) > 7.4 \cdot 10^{-4}$ W.u., $B(M1) > 0.031$ W.u., and $B(E2) > 371$ W.u. for the 468-keV decay and $B(E1) > 2.6 \cdot 10^{-3}$ W.u., $B(M1) > 0.11$ W.u., and
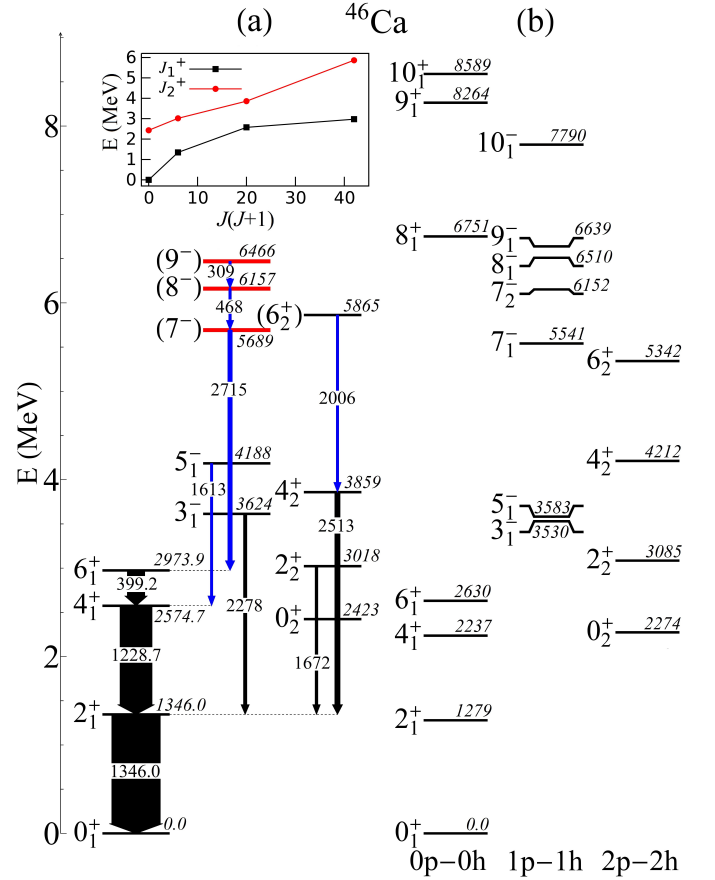

FIG. 5. Experimental level scheme of ^{46}Ca (a) compared to results of $sd - pf - sdg$ shell model calculations (b). Excited states (gamma-ray transitions) newly identified from this work are shown in red (blue). The inset shows excitation energy vs. angular momentum for the yrast J_1^+ (black) and yrare J_2^+ (red) bands, where the lines are to guide the eyes.

$B(E2) > 2960$ W.u. for the 309-keV decay. According to recommended upper limits for the A=45-90 region [42], which are given as 0.01, 3, and 300 W.u. for E1, M1, and E2 respectively, the cascade decay should predominantly occur via either E1 or M1 transitions. These observations prompt two possible assignments: $(9) \rightarrow (8) \rightarrow (7)$ or $(10) \rightarrow (9) \rightarrow (8)$, as discussed further below.

Figure 5(b) presents the result of the large-scale shell model calculation in the $sd - pf - sdg$ valence space including cross-shell excitations for negative-parity one-particle-one-hole (1p-1h) states as well as positive-parity 0p-0h and 2p-2h states, without mixing across configurations. The SDPF-MU interaction [43] with the modification found in Ref. [6] was used. Electromagnetic strengths were calculated using effective charges $(e_p, e_n) = (1.5e, 0.5e)$ and effective $g_s' = 0.7g_s$ and $g_l' = 1.0g_l$ modified from bare g values.

The present calculations for the 0p-0h states shown in Fig. 5(b) are essentially the same as the results from an fp-shell shell model calculation using the GXPF1A

TABLE I. The levels of ^{46}Ca identified in this experiment. Intensity (I_γ) is presented relative to the 1346-keV gamma-ray yield and is corrected by a scaling factor that accounts for differences in gamma-ray efficiencies [40] as well as effective target thickness available for each reaction channel. New results from this experiment are in bold, others are in agreement with accepted ENSDF values [41].

E_{initial} (keV)	J^π	E_γ (keV)	E_{final} (keV)	I_γ
1346.0(5)	2_1^+	1346.0(5)	0	100
2574.7(7)	4_1^+	1228.7(5)	1346.0	65.9(6)
2973.9(9)	6_1^+	399.2(5)	2474.7	35.7(6)
3018(3)	2_2^+	1672(3)	1346.0	3.0(19)
3624(4)	3_1^-	2278(4)	1346.0	6.5(10)
3859(3)	4_2^+	2513(3)	1346.0	10.8(14)
4188(3)	5_1^-	**1613(3)**	2574.7	4.8(7)
5689(2)	(7^-)	**2715(2)**	2973.9	9.2(14)
5865(5)	(6_2^+)	**2006(3)**	3859	5.1(11)
6157(3)	(8^-)	**468(2)**	5689	4.5(6)
6466(4)	(9^-)	**309(2)**	6157	5.7(8)

Hamiltonian. However, the predicted locations of the 8_1^+-10_1^+ states are much higher than the cascade of transitions newly observed in this work. The broad reliability of GXPF1A to accurately reproduce high-spin yrast level energies is well-established [44], so this discrepancy with the observed level spacing does not support a $10_1^+ \rightarrow 9_1^+ \rightarrow 8_1^+$ assignment, though it is not completely ruled out by the present data. If one looks at the results for the 1p-1h and 2p-2h excitations, the observed levels were more consistent with the $(9^-) \rightarrow (8^-) \rightarrow (7^-)$ cascade transition. In particular, the $8_1^- \rightarrow 7_2^-$ transition is predicted to have an M1 strength of $B(M1) = 0.57$ W.u., consistent with the experimental lower limit of 0.031 W.u.. The other $8_1^- \rightarrow 7_1^-$ transition is less likely to correspond because its predicted transition strength of 0.030 W.u. is close to the conservative lower limit. Similarly, the predicted strength of $B(M1) = 0.16$ W.u. for the $9_1^- \rightarrow 8_1^-$ transition is consistent with the experimental lower limit of 0.11 W.u. This suggests that the observed cascade corresponds to the $9_1^- \rightarrow 8_1^- \rightarrow 7_2^-$ shell model levels.

The behavior of the band-like structures illustrated in Fig. 5 can be studied by comparisons to neighboring nuclei as well as with shell model calculations. For the negative-parity band, the observed $(9^-) \rightarrow (8^-) \rightarrow (7^-)$ cascade in ^{46}Ca has a much smaller level spacing as compared to the $(7^-) \rightarrow 5^-$ energy difference, and does not follow the increasing $J(J+1)$ level spacing as observed for the rotational-like negative-parity band in ^{44}Ca. In the case of ^{44}Ca, strong E2 transitions are observed among the negative-parity states, whereas the 3_1^-, 5_1^-, and (7^-) states in ^{46}Ca appear to primarily decay by E1 transitions to the yrast band, suggesting a particle-hole character for these states. This view is also supported by the large gap between the 5_1^- and (7^-) states, which is comparable to that observed for the 0_{gs}^+ and other yrast levels, because 5_1^- can be formed as the $(d_{3/2}^{-1})(f_{7/2}^1)$ spin-stretched state coupled to 0_{gs}^+, whereas the (7^-) state requires core excitations.

On the other hand, it should be noted that the $(6_2^+) \rightarrow 4_2^+$ gamma transition energy was found to follow the $J(J+1)$ trend expected for a rotational band (Fig. 5

inset), confirming the deformed band structure on top of the 0_2^+ state. The shell model calculations show a somewhat compressed band structure; however, they predict large $B(E2)$ values within the yrare band (26.3, 35.2, and 32.0 W.u. for the 2_2^+, 4_2^+, and 6_2^+ decays, respectively), suggesting substantial collectivity. The present calculations also show dominant proton 2p-2h excitations in these yrare states. These results indicate the prevalence of shape coexistence in ^{46}Ca formed by the different particle-hole (0p-0h and 2p-2h) configurations, confirming the transition of 0_2^+ bands (suggested in Ref. [19]) from dominant 4p-4h (6p-4h) configurations in ^{40}Ca (^{42}Ca) to proton 2p-2h excitations.

In summary, we demonstrated the usefulness of fusion evaporation reactions when combined with reaccelerated rare isotope beams to access unexplored high-spin states in the neutron-rich regime with gamma-ray spectroscopy. Three new states and five new transitions were observed in ^{46}Ca. Together with the consistency with the large-scale shell model calculations, the present results suggest the persistence of shape coexistence in ^{46}Ca due to the competition between established shell structure and particle-hole excitations. This work opens the way for further investigation into more neutron-rich Ca isotopes away from stability, where new magicity has recently been identified.

[1] G. Hagen, M. Hjorth-Jensen, G. R. Jansen, R. Machleidt, and T. Papenbrock, Phys. Rev. Lett. **109**, 032502 (2012).

[2] J. Erler, N. Birge, M. Kortelainen, W. Nazarewicz, E. Olsen, A. M. Perhac, and M. Stoitsov, Nature **486**, 509 (2012).

[3] O. B. Tarasov, D. S. Ahn, D. Bazin, N. Fukuda, A. Gade, M. Hausmann, N. Inabe, S. Ishikawa, N. Iwasa, K. Kawata, T. Komatsubara, T. Kubo, K. Kusaka, D. J. Morrissey, M. Ohtake, H. Otsu, M. Portillo, T. Sakakibara, H. Sakurai, H. Sato, B. M. Sherrill, Y. Shimizu, A. Stolz, T. Sumikama, H. Suzuki, H. Takeda, M. Thoennessen, H. Ueno, Y. Yanagisawa, and K. Yoshida, Phys. Rev. Lett. **121**, 022501 (2018).

[4] A. Huck, G. Klotz, A. Knipper, C. Miehé, C. Richard-Serre, G. Walter, A. Poves, H. L. Ravn, and G. Marguier, Phys. Rev. C **31**, 2226 (1985).

[5] A. Gade, R. V. F. Janssens, D. Bazin, R. Broda, B. A. Brown, C. M. Campbell, M. P. Carpenter, J. M. Cook, A. N. Deacon, D.-C. Dinca, B. Fornal, S. J. Freeman, T. Glasmacher, P. G. Hansen, B. P. Kay, P. F. Mantica, W. F. Mueller, J. R. Terry, J. A. Tostevin, and S. Zhu, Phys. Rev. C **74**, 021302(R) (2006).

[6] D. Steppenbeck, S. Takeuchi, N. Aoi, P. Doornenbal, M. Matsushita, H. Wang, H. Baba, N. Fukuda, S. Go, M. Honma, J. Lee, K. Matsui, S. Michimasa, T. Motobayashi, D. Nishimura, T. Otsuka, H. Sakurai, Y. Shiga,

P.-A. Söderström, T. Sumikama, H. Suzuki, R. Taniuchi, Y. Utsuno, J. J. Valiente-Dobón, and K. Yoneda, Nature **502**, 207 (2013).

[7] F. Wienholtz, D. Beck, K. Blaum, C. Borgmann, M. Breitenfeldt, R. B. Cakirli, S. George, F. Herfurth, J. D. Holt, M. Kowalska, S. Kreim, D. Lunney, V. Manea, J. Menéndez, D. Neidherr, M. Rosenbusch, L. Schweikhard, A. Schwenk, J. Simonis, J. Stanja, R. N. Wolf, and K. Zuber, Nature **498**, 346 (2013).

[8] S. Michimasa, M. Kobayashi, Y. Kiyokawa, S. Ota, D. S. Ahn, H. Baba, G. P. A. Berg, M. Dozono, N. Fukuda, T. Furuno, E. Ideguchi, N. Inabe, T. Kawabata, S. Kawase, K. Kisamori, K. Kobayashi, T. Kubo, Y. Kubota, C. S. Lee, M. Matsushita, H. Miya, A. Mizukami, H. Nagakura, D. Nishimura, H. Oikawa, H. Sakai, Y. Shimizu, A. Stolz, H. Suzuki, M. Takaki, H. Takeda, S. Takeuchi, H. Tokieda, T. Uesaka, K. Yako, Y. Yamaguchi, Y. Yanagisawa, R. Yokoyama, K. Yoshida, and S. Shimoura, Phys. Rev. Lett. **121**, 022506 (2018).

[9] R. F. Garcia Ruiz, M. L. Bissell, K. Blaum, A. Ekström, N. Frömmgen, G. Hagen, M. Hammen, K. Hebeler, J. D. Holt, G. R. Jansen, M. Kowalska, K. Kreim, W. Nazarewicz, R. Neugart, G. Neyens, W. Nörtershäuser, T. Papenbrock, J. Papuga, A. Schwenk, J. Simonis, K. . A. Wendt, and D. T. Yordanov, Nature Physics **12**, 594 (2016).

[10] A. J. Miller, K. Minamisono, A. Klose, D. Garand, C. Kujawa, J. D. Lantis, Y. Liu, B. Maaß, P. F. Mantica, W. Nazarewicz, W. Nörtershäuser, S. V. Pineda, P.-G. Reinhard, D. M. Rossi, F. Sommer, C. Sumithrarachchi, A. Teigelhöfer, and J. Watkins, Nature Physics **15**, 432 (2019).

[11] G. D. Dracoulis, A. P. Byrne, T. Kibédi, T. R. McGoram, and S. M. Mullins, Journal of Physics G: Nuclear and Particle Physics **23**, 1191 (1997).

[12] J. J. Valiente-Dobón, S. M. Lenzi, S. J. Freeman, S. Lunardi, J. F. Smith, A. Gottardo, F. DellaVedova, E. Farnea, A. Gadea, D. R. Napoli, M. Axiotis, S. Aydin, D. Bazzacco, P. G. Bizzeti, A. M. Bizzeti-Sona, G. Benzoni, D. Bucurescu, L. Corradi, A. N. Deacon, A. de Angelis, E. Fioretto, B. Guiot, M. Ionescu-Bujor, A. Iordachescu, S. Leoni, N. Marginean, R. Marginean, P. Mason, R. Menegazzo, D. Mengoni, B. Million, G. Montagnoli, R. Orlandi, F. Recchia, E. Sahin, F. Scarlassara, R. P. Singh, A. M. Stefanini, D. Steppenbeck, S. Szilner, C. A. Ur, B. J. Varley, and O. Wieland, Phys. Rev. C **78**, 024302 (2008).

[13] E. Ideguchi, Progress of Theoretical and Experimental Physics **2012** (2012), 10.1093/ptep/pts040, 03C005.

[14] S. Zhu, R. V. F. Janssens, B. Fornal, S. J. Freeman, M. Honma, R. Broda, M. P. Carpenter, A. N. Deacon, E. Jackson, B. P. Kay, T. Lauritsen, C. J. Lister, P. F. Mantica, T. Otsuka, D. Seweryniak, J. F. Smith, D. Steppenbeck, and X. Wang, Phys. Rev. C **80**, 024318 (2009).

[15] S. Bottoni, S. Leoni, B. Fornal, R. Raabe, K. Rusek, G. Benzoni, A. Bracco, F. C. L. Crespi, A. I. Morales, P. Bednarczyk, N. Cieplicka-Oryńczak, W. Królas, A. Maj, B. Szpak, M. Callens, J. Bouma, J. Elseviers, H. De Witte, F. Flavigny, R. Orlandi, P. Reiter, M. Seidlitz, N. Warr, B. Siebeck, S. Hellgartner, D. Mücher, J. Pakarinen, M. Vermeulen, C. Bauer, G. Georgiev, R. V. F. Janssens, D. Balabanski, M. Sferrazza, M. Kowalska, E. Rapisarda, D. Voulot, M. Lozano Benito, and F. Wenander, Phys. Rev. C **92**, 024322 (2015).

[16] E. Ideguchi, D. G. Sarantites, W. Reviol, A. V. Afanasjev, M. Devlin, C. Baktash, R. V. F. Janssens, D. Rudolph, A. Axelsson, M. P. Carpenter, A. Galindo-Uribarri, D. R. LaFosse, T. Lauritsen, F. Lerma, C. J. Lister, P. Reiter, D. Seweryniak, D. Weiszflog, and J. N. Wilson, Phys. Rev. Lett. **87**, 222501 (2001).

[17] K. Hadyńska-Klęk, P. J. Napiorkowski, M. Zielińska, J. Srebrny, A. Maj, F. Azaiez, J. J. Valiente Dobón, M. Kici ńska Habior, H. Nowacki, H. Naïdja, B. Bounthong, T. R. Rodríguez, G. de Angelis, T. Abraham, G. Anil Kumar, D. Bazzacco, M. Bellato, D. Bortolato, P. Bednarczyk, G. Benzoni, L. Berti, B. Birkenbach, B. Bruyneel, S. Brambilla, F. Camera, J. Chavas, B. Cederwall, L. Charles, M. Ciemała, P. Cocconi, P. Coleman-Smith, A. Colombo, A. Corsi, F. C. L. Crespi, D. M. Cullen, A. Czermak, P. Désesquelles, D. T. Doherty, B. Dulny, J. Eberth, E. Farnea, B. Fornal, S. Franchoo, A. Gadea, A. Giaz, A. Gottardo, X. Grave, J. Grębosz, A. Görgen, M. Gulmini, T. Habermann, H. Hess, R. Isocrate, J. Iwanicki, G. Jaworski, D. S. Judson, A. Jungclaus, N. Karkour, M. Kmiecik, D. Karpiński, M. Kisieliński, N. Kondratyev, A. Korichi, M. Komorowska, M. Kowalczyk, W. Korten, M. Krzysiek, G. Lehaut, S. Leoni, J. Ljungvall, A. Lopez-Martens, S. Lunardi, G. Maron, K. Mazurek, R. Menegazzo, D. Mengoni, E. Merchán, W. Męczyński, C. Michelagnoli, J. Mierzejewski, B. Million, S. Myalski, D. R. Napoli, R. Nicolini, M. Niikura, A. Obertelli, S. F. Özmen, M. Palacz, L. Próchniak, A. Pullia, B. Quintana, G. Rampazzo, F. Recchia, N. Redon, P. Reiter, D. Rosso, K. Rusek, E. Sahin, M.-D. Salsac, P.-A. Söderström, I. Stefan, O. Stézowski, J. Styczeń, C. Theisen, N. Toniolo, C. A. Ur, V. Vandone, R. Wadsworth, B. Wasilewska, A. Wiens, J. L. Wood, K. Wrzosek-Lipska, and M. Ziębliński, Phys. Rev. Lett. **117**, 062501 (2016).

[18] M. Lach, P. Bednarczyk, A. Bracco, J. Grebosz, M. Kadluczka, N. Kintz, A. Maj, J. C. Merdinger, W. Meczynski, J. L. Pedroza, N. Schulz, M. B. Smith, K. M. Spohr, J. Styczen, J. P. Vivien, and M. Zieblinski, The European Physical Journal A - Hadrons and Nuclei **12**, 381 (2001).

[19] J. Wood, K. Heyde, W. Nazarewicz, M. Huyse, and P. van Duppen, Physics Reports **215**, 101 (1992).

[20] B. A. Brown, Physics **3**, 104 (2010).

[21] R. Taniuchi, C. Santamaria, P. Doornenbal, A. Obertelli, K. Yoneda, G. Authelet, H. Baba, D. Calvet, F. Château, A. Corsi, A. Delbart, J.-M. Gheller, A. Gillibert, J. D. Holt, T. Isobe, V. Lapoux, M. Matsushita, J. Menéndez, S. Momiyama, T. Motobayashi, M. Niikura, F. Nowacki, K. Ogata, H. Otsu, T. Otsuka, C. Péron, S. Péru, A. Peyaud, E. C. Pollacco, A. Poves, J.-Y. Roussé, H. Sakurai, A. Schwenk, Y. Shiga, J. Simonis, S. R. Stroberg, Y. Tsunoda, T. Uesaka, H. Wang, F. Browne, L. X. Chung, Z. Dombradi, S. Franchoo, F. Giacoppo, A. Gottardo, K. Hadyńska-Klęk, Z. Korkulu, S. Koyama, Y. Kubota, J. Lee, M. Lettmann, C. Louchart, R. Lozeva, K. Matsui, T. Miyazaki, S. Nishimura, L. Olivier, S. Ota, Z. Patel, E. Şahin, C. Shand, P.-A. Söderström, I. Stefan, D. Steppenbeck, T. Sumikama, D. Suzuki, Z. Vajta, V. Werner, J. Wu, and Z. Y. Xu, Nature **569**, 53 (2019).

[22] F. Nowacki, A. Poves, E. Caurier, and B. Bounthong, Phys. Rev. Lett. **117**, 272501 (2016).

[23] Y. Iwata, N. Shimizu, T. Otsuka, Y. Utsuno, J. Menén-dez, M. Honma, and T. Abe, Phys. Rev. Lett. **116**, 112502 (2016).

[24] T. R. Rodríguez and J. L. Egido, Phys. Rev. Lett. **99**, 062501 (2007).

[25] L. Coraggio, A. Covello, A. Gargano, and N. Itaco, Phys. Rev. C **80**, 044311 (2009).

[26] J. Bjerregaard, O. Hansen, O. Nathan, R. Chapman, S. Hinds, and R. Middleton, Nuclear Physics A **103**, 33 (1967).

[27] G. M. Crawley, P. S. Miller, G. J. Igo, and J. Kulleck, Phys. Rev. C **8**, 574 (1973).

[28] W. W. Daehnick and M. J. Spisak, Phys. Rev. C **7**, 2593 (1973).

[29] D. Montanari, S. Leoni, D. Mengoni, J. J. Valiente-Dobon, G. Benzoni, N. Blasi, G. Bocchi, P. F. Bor-tignon, S. Bottoni, A. Bracco, F. Camera, P. Casati, G. Colò, A. Corsi, F. C. L. Crespi, B. Million, R. Nicol-ini, O. Wieland, D. Bazzacco, E. Farnea, G. Germogli, A. Gottardo, S. M. Lenzi, S. Lunardi, R. Menegazzo, G. Montagnoli, F. Recchia, F. Scarlassara, C. Ur, L. Cor-radi, G. de Angelis, E. Fioretto, D. R. Napoli, R. Orlandi, E. Sahin, A. M. Stefanini, R. P. Singh, A. Gadea, S. Szil-ner, M. Kmiecik, A. Maj, W. Meczynski, A. Dewald, T. Pissulla, and G. Pollarolo, Phys. Rev. C **85**, 044301 (2012).

[30] J. L. Pore, C. Andreoiu, J. K. Smith, A. D. MacLean, A. Chester, J. D. Holt, G. C. Ball, P. C. Bender, V. Bild-stein, R. Braid, A. Diaz Varela, R. Dunlop, L. J. Evitts, A. B. Garnsworthy, P. E. Garrett, G. Hackman, S. V. Ilyushkin, B. Jigmeddorj, K. Kuhn, P. Kunz, A. T. Laf-foley, K. G. Leach, D. Miller, W. J. Mills, W. Moore, M. Moukaddam, L. N. Morrison, B. Olaizola, E. E. Pe-ters, A. J. Radich, E. T. Rand, F. Sarazin, D. Southall, C. E. Svensson, S. J. Williams, and S. W. Yates, Phys. Rev. C **100**, 054327 (2019).

[31] D. Morrissey, B. Sherrill, M. Steiner, A. Stolz, and I. Wiedenhoever, Nuclear Instruments and Methods in Physics Research Section B: Beam Interactions with Ma-terials and Atoms **204**, 90 (2003), 14th International Conference on Electromagnetic Isotope Separators and Techniques Related to their Applications.

[32] A. Villari, D. Alt, G. Bollen, D. Crisp, M. Ikegami, S. Krause, A. Lapierre, S. Lidia, D. Morrissey, S. Nash, R. Rencsok, R. Ringle, S. Schwarz, R. Shane, C. Sum-ithrarachchi, S. Williams, and Q. Zhao, *Commissioning and First Accelerated Beams in the Reaccelerator (Rea3) of the National Superconducting Cyclotron Laboratory, MSU* (Busan, Korea) pp. 1287–1290.

[33] A. Lapierre, G. Bollen, J. R. C. Lopez-Urrutia, M. Doleans, S. Geyer, O. Kester, K. Kittimanapun, M. Portillo, and S. Schwarz, Journal of Instrumentation **5**, c07001 (2010).

[34] A. Gavron, Phys. Rev. C **21**, 230 (1980).

[35] W. Mueller, J. Church, T. Glasmacher, D. Gutknecht, G. Hackman, P. Hansen, Z. Hu, K. Miller, and P. Quirin, Nuclear Instruments and Methods in Physics Research Section A: Accelerators, Spectrometers, Detectors and Associated Equipment **466**, 492 (2001).

[36] J. F. Ziegler, M. Ziegler, and J. Biersack, Nuclear Instru-ments and Methods in Physics Research Section B: Beam Interactions with Materials and Atoms **268**, 1818 (2010), 19th International Conference on Ion Beam Analysis.

[37] E. Lunderberg, J. Belarge, P. Bender, B. Bucher, D. Cline, B. Elman, A. Gade, S. Liddick, B. Longfel-low, C. Prokop, D. Weisshaar, and C. Wu, Nuclear In-struments and Methods in Physics Research Section A: Accelerators, Spectrometers, Detectors and Associated Equipment **885**, 30 (2018).

[38] P. G. Bizzeti, P. R. Maurenzig, G. Poggi, and G. Lo Bianco, Lett.Nuovo Cim. **12**, 53 (1975).

[39] W. Kutschera, B. A. Brown, H. Ikezoe, G. D. Sprouse, Y. Yamazaki, Y. Yoshida, T. Nomura, and H. Ohnuma, Phys. Rev. C **12**, 813 (1975).

[40] A. Lemasson, H. Iwasaki, C. Morse, D. Bazin, T. Baugher, J. S. Berryman, A. Dewald, C. Fransen, A. Gade, S. McDaniel, A. Nichols, A. Ratkiewicz, S. Stroberg, P. Voss, R. Wadsworth, D. Weisshaar, K. Wimmer, and R. Winkler, Phys. Rev. C **85**, 041303(R) (2012).

[41] S.-C. Wu, Nuclear Data Sheets **91**, 1 (2000).

[42] P. Endt, Atomic Data and Nuclear Data Tables **23**, 547 (1979).

[43] Y. Utsuno, T. Otsuka, B. A. Brown, M. Honma, T. Mizusaki, and N. Shimizu, Phys. Rev. C **86**, 051301(R) (2012).

[44] M. Honma, T. Otsuka, B. A. Brown, and T. Mizusaki, Phys. Rev. C **69**, 034335 (2004).